

UNIVERSIDADE ESTADUAL DE CAMPINAS
SISTEMA DE BIBLIOTECAS DA UNICAMP
REPOSITÓRIO DA PRODUÇÃO CIENTÍFICA E INTELLECTUAL DA UNICAMP

Versão do arquivo anexado / Version of attached file:

Versão do Editor / Published Version

Mais informações no site da editora / Further information on publisher's website:

<https://www.sciencedirect.com/science/article/pii/S0022231314002361>

DOI: 10.1016/j.jlumin.2014.03.071

Direitos autorais / Publisher's copyright statement:

©2014 by Elsevier. All rights reserved.

DIRETORIA DE TRATAMENTO DA INFORMAÇÃO

Cidade Universitária Zeferino Vaz Barão Geraldo

CEP 13083-970 – Campinas SP

Fone: (19) 3521-6493

<http://www.repositorio.unicamp.br>



The influence of carboxylate, phosphinate and seleninate groups on luminescent properties of lanthanides complexes

Jorge H.S.K. Monteiro, André L.B. Formiga, Fernando A. Sigoli*

Laboratory of Functional Materials – Institute of Chemistry, University of Campinas – Unicamp, Campinas, SP 13083-970, Brazil

ARTICLE INFO

Article history:

Received 2 October 2013

Received in revised form

24 March 2014

Accepted 31 March 2014

Available online 13 April 2014

Keywords:

Lanthanide

Complexes

Luminescence

Energy transfer rates

Quantum yield

ABSTRACT

The lanthanides(III) complexes $[\text{Ln}(\text{bza})_3(\text{H}_2\text{O})_n] \cdot m\text{H}_2\text{O}$, $[\text{Ln}(\text{ppa})_3(\text{H}_2\text{O})_n] \cdot m\text{H}_2\text{O}$ and $[\text{Ln}(\text{abse})_3(\text{H}_2\text{O})_n] \cdot m\text{H}_2\text{O}$ where $\text{Ln} = \text{Eu}^{3+}$, Gd^{3+} or Tb^{3+} were synthesized using sodium benzoate (Nabza), sodium phenylseleninate (Naabse) and sodium phenylphosphinate (Nappa) in order to verify the influence on coordination modes and the luminescence parameters when the carbon is exchanged by phosphorus or selenium in those ligands. The complexes' stoichiometries were determined by lanthanide(III) titration, microanalysis and TGA. The coordination modes were determined as bidentate bridging and chelate by the FT-IR. The triplet state energies of the ligands were obtained by two different approaches giving a difference of about $\sim 2000 \text{ cm}^{-1}$ between them. The $[\text{Eu}(\text{abse})_3(\text{H}_2\text{O})]$ complex shows the higher degree of covalence which was verified by the centroid of $^5\text{D}_0 \rightarrow ^7\text{F}_0$ transition ($17,248 \text{ cm}^{-1}$). On the other hand the $[\text{Ln}(\text{abse})_3(\text{H}_2\text{O})_n] \cdot m\text{H}_2\text{O}$ complexes have an inefficient antenna effect verified by the low values of absolute emission quantum yields. The $[\text{Ln}(\text{ppa})_3(\text{H}_2\text{O})_n] \cdot m\text{H}_2\text{O}$ complexes have higher emission decay lifetime values among the complexes which is a result of the ability of this ligand to form coordination polymers avoiding water molecules in the first coordination sphere. The $[\text{Eu}(\text{ppa})_3]$ complex has the highest point symmetry around europium(III) among the synthesized complexes, followed by the $[\text{Eu}(\text{bza})_3(\text{H}_2\text{O})_2] \cdot 3/2(\text{H}_2\text{O})$ and $[\text{Eu}(\text{abse})_3(\text{H}_2\text{O})]$ complexes where europium(III) show similar point symmetries. As one may expect, the triplet state energy position would change the transfer and/or back energy transfer rates from ligand to metal. The calculation of these rates show that the back energy transfer rates are more affected than the transfer ones by changing the triplet state energy in the range of $\sim 2000 \text{ cm}^{-1}$. The changes in the energy transfer rates from triplet state to europium(III) levels are not sufficient to significantly modify the population of the europium(III) $^5\text{D}_{0,1}$ levels and therefore the emission quantum yield.

© 2014 Elsevier B.V. All rights reserved.

1. Introduction

The most part of lanthanides(III)-doped materials can be applied in several fields such as: displays, sensors, biomarkers, etc. [1–3] due to their luminescent properties. The lanthanides(III) emission may happen from the visible (Tb^{3+} and Eu^{3+} , for example) to near infrared regions (Nd^{3+} and Er^{3+} , for example). The emission spectra of lanthanides(III)-doped compounds are composed by narrow bands due to the intraconfigurational 4f–4f transitions that are forbidden by Laporte's rule and in some cases they are also forbidden by Spin's rule. The presence of a non-symmetric electric field around lanthanide(III) ions due to inorganic or organic ligands [1–3] promotes the mixing of electronic states with opposite parities relaxing Laporte's rule. The complexes containing organic ligands are interesting for academic

studies and applications because the ligands play an important role in the properties of the complex such as: stability, solubility, interactions with biological groups and also emission efficiency. The energy pathway (excitation to emission) in lanthanide(III) complexes is a tricky process which involves energy transfer and back transfer rates between ligand states and lanthanide levels. The excitation may occur through the ligand states (fundamental to excited singlet states) followed by intersystem crossing (energy transfer from excited singlet to triplet states), energy transfer from ligand to lanthanide(III) excited levels and finally the emission occurs through the lanthanide f–f transitions, according to the traditional energy transfer from triplet states to lanthanide. The energy transfer also may happen via charge transfer or even directly from the excited singlet state; in both cases the energy transfer from the triplet state is ruled out [4,5]. The emission efficiency of the lanthanide(III) complex depends on: (i) the energy of the triplet state that should be above the lanthanide ion emitting level [4,6], being 2500 cm^{-1} desirable in order to decrease the back energy transfer rate; (ii) the non-radiative

* Corresponding author.

E-mail address: fsigoli@iqm.unicamp.br (F.A. Sigoli).

processes that are usually caused by the presence of O–H, N–H and C–H oscillators; (iii) the ligand field asymmetry and (iv) the transfer and back energy transfer rates between the ligand and the lanthanide ion [1,6].

Among several organic ligands used for preparing complexes of lanthanide(III) ions, the ligands containing the carboxylates are widely reported in the literature [7,8]. There are several reports concerning the structure as well as some luminescent properties of complexes containing this kind of ligand. The carboxylate ion may coordinate to the lanthanide(III) by several coordination modes such as: bidentate bridging, bidentate chelate, monodentate or mixed modes like bridging and chelate [7,8]. Ligands containing phosphinate and seleninate groups are not often reported in the literature. The lanthanide(III) complexes containing diphenylphosphinate (dpp) as coordination group were reported by Stucchi and co-workers [9,10]. The latter ligand has the ability to form stable bonds with lanthanides(III) ions and usually its lanthanide(III) complexes do not have water molecules in the first coordination sphere [9,10]. Malta and co-workers [11] reported on the synthesis and spectroscopic characterization of two lanthanide(III) complexes containing the ligands benzeneseleninic acid (abse) and 4-chloro-benzeneseleninic acid (abseCl). These authors reported on the influence of the addition of chlorine in the phenyl ring on the covalence of Ln–O bonds but did not explore the possible different coordination modes of the seleninate group. There is no report in the literature comparing the changes caused by the replacement of the carbon by phosphorus or selenium in a specific ligand molecular structure. The understanding of how the carboxylates, phosphinates or seleninates groups may change the chemical nature of coordination sphere, the point symmetry around lanthanide ions and the luminescent properties is important in order to plan futures complexes that show desirable properties, such as high emission quantum yields.

The present work reports on possible changes of coordination modes and luminescent properties of lanthanides(III) complexes originated from the replacement of the carbon atom of a carboxylate ligand for selenium or phosphorus. The ligands benzoic acid (bza), phenylseleninic acid (abse) and phenylphosphinic acid (ppa) were chosen to study the influence of those different atoms on the complexes' chemical stoichiometries, coordination polyhedron, number of coordinated water molecules and energies of ligands' excited states. Theoretical Judd–Ofelt (JO) intensity parameters, energy transfer rates and the emission quantum yield were theoretically estimated using data of polar spherical coordinates of atoms of the complexes in the ground state geometries that were obtained from semi-empirical methods: Sparkle/AM1, Sparkle/PM3 and Sparkle/PM6. In order to evaluate the ground state geometry of the lanthanides(III) complexes the theoretical values of JO parameters were compared to the experimental ones. The influence of those ligands on the nature of chemical bonds between the oxygen and the lanthanides(III) ions is discussed as well.

2. Experimental section

The complexes were synthesized as follows: sodium hydroxide (NaOH) in a molar ratio 1:1 (L:OH), was added drop by drop in aqueous suspensions of the respective ligands (L = bza, abse and ppa) under stirring during 30 min at 70 °C. The complete dissolution of the ligands was an indicative of formation of their respective sodium salts. The aqueous solutions of the ligands' salts were separately added to an aqueous solution of lanthanide ($\text{Ln}^{3+} = \text{Eu}^{3+}$, Gd^{3+} or Tb^{3+}) ions, with a pH value equal to 5.0, in a molar ratio 3:1 (L: Ln^{3+}). A white precipitate was formed immediately for all ligands. The complexes' suspensions were

stirred during 90 min at 80 °C for complete precipitation. After that time the solids were kept resting for 1 h, followed by filtration and washed with several portions of hot water. The solids were placed into a desiccator containing silica.

3. Characterizations

The chemical stoichiometries of the complexes were suggested by Ln^{3+} titration using a standard 0.01 mol L^{−1} EDTA solution, carbon and hydrogen microanalysis (Perkin Elmer 2400) and thermogravimetric analysis (TA instruments SDTQ600) that were carried out using a dynamic synthetic air atmosphere (100 mL min^{−1}) under a heating rate of 10 °C min^{−1}. Infrared spectroscopy (FT-IR Bomem FT/IR 2000) data were obtained in transmission mode using KBr pellets.

The photoluminescence data were obtained in a Fluorolog-3 spectrofluorometer (Horiba FL3-22-iHR320), with double-gratings (1200 g/mm, 330 nm blazed) in the excitation monochromator and double-gratings (1200 g/mm, 500 nm blazed) in the emission monochromator. An ozone-free Xenon lamp of 450 W (Ushio) was used as a radiation source. The excitation spectra were obtained between 200–600 nm and they were corrected in real time according to the lamp intensity and the optical system of the excitation monochromator using a silicon diode as a reference. The emission spectra were carried out between 400–750 nm using the front face mode at 22.5°. All of them were corrected according to the optical system of the emission monochromator and the photomultiplier response (Hamamatsu R928P). The time resolved emission spectra were measured using a phosphorimeter system with a delay of 0.5 ms, in order to get only the emissions from triplet states of the ligands. The emission decay curves were obtained with a pulsed 150 W Xenon lamp using a phosphorimeter. The absolute quantum yields were measured using a Quanta-φ (Horiba F-309) integrating sphere equipped with an optical-fibers bundle (NA=0.22-Horiba-FL-3000/FM4-3000).

4. Determination of ground state geometries

For the determination of the complexes' ground state geometries the lanthanide ion was replaced by a +3e point charge [12–14], the RHF wavefunctions were optimized using the Broyden–Fletcher–Goldfarb–Shanno procedure with a convergence criterion of 0.01 kcal mol^{−1} Å^{−1}, semi empiricals AM1 or PM3 or PM6 with a convergence criteria of 10^{−6} kcal mol^{−1} for the SCF. In Mopac2009 package [15] the following keywords were used: MODEL (AM1, PM3 or PM6), SPARKLE, XYZ, SCFCRT=1D-10, GEO-OK, BFGS, CHARGE=X, PRECISE, GNORM=0.10 and T=1D.

5. Results and discussion

As the first characterization the chemical formulae of the complexes were suggested from titration, carbon and hydrogen microanalysis. The results are shown in Table 1.

The amount of water molecules coordinated to the lanthanide ions were checked by thermogravimetric analysis (TGA). The TG curves are shown in the ESI (Fig. S1). The weight loss attributed to loss of water molecules coordinated to lanthanides(III) ions was calculated and determined experimentally from the TG data using the temperature range from 80–200 °C (Table 2).

Once the complexes' stoichiometries were determined the coordination modes of the ligand bza[−] were suggested by FT-IR and $\Delta\nu$, where $\Delta\nu = \nu_{\text{as}}(\text{COO}^-) - \nu_{\text{s}}(\text{COO}^-)$ [16,17]. The carboxylate coordination in complexes can be by several modes, such as: monodentate, bidentate bridging and/or bidentate chelate. For

Table 1
Results of the Ln^{3+} titration and carbon and hydrogen microanalysis for all complexes obtained.

Complexes	% Ln^{3+} calc	% Ln^{3+} exp	% C calc	% C exp	% H calc	% H exp
[Eu(bza) ₃ (H ₂ O) ₂] · 3/2(H ₂ O)	26.3	25.4	44.61	45.43	3.83	3.45
[Eu(ppa) ₃]	26.4	25.8	37.59	37.64	3.15	3.17
[Eu(abse) ₃ (H ₂ O)]	20.7	20.3	29.45	28.51	2.33	2.32
[Gd(bza) ₃] · (H ₂ O)	29.2	27.8	46.83	47.17	3.18	3.07
[Gd(ppa) ₃]	27.1	26.3	37.24	37.15	3.13	3.11
[Gd(abse) ₃] · (H ₂ O)	21.3	22.5	29.24	28.42	2.32	2.31
[Tb(bza) ₃ (H ₂ O) ₂] · 1/2(H ₂ O)	28.0	26.9	44.46	43.28	3.55	3.77
[Tb(ppa) ₃]	27.3	25.5	37.14	36.84	3.11	3.07
[Tb(abse) ₃ (H ₂ O)]	21.8	21.4	29.17	30.41	2.31	2.71

Table 2
Amount of coordinated water molecules calculated and determined experimentally.

Complexes	(Δm) _{exp} (%)	(Δm) _{calc} (%)
[Eu(bza) ₃ (H ₂ O) ₂] · 3/2(H ₂ O)	10.48	10.89
[Eu(abse) ₃ (H ₂ O)]	2.78	3.29
[Eu(ppa) ₃]	0	0
[Gd(bza) ₃] · (H ₂ O)	3.34	3.20
[Gd(abse) ₃] · (H ₂ O)	3.02	2.43
[Gd(ppa) ₃]	0	0
[Tb(bza) ₃ (H ₂ O) ₂] · 1/2(H ₂ O)	7.50	7.93
[Tb(abse) ₃ (H ₂ O)]	2.65	2.43
[Tb(ppa) ₃]	0	0

each of the cases mentioned above the $\Delta\nu$ value of the complex can be higher, nearly the same or lower than the $\Delta\nu$ of the ligand salt. For the monodentate mode the $\Delta\nu$ of complex is greater than the value of $\Delta\nu$ of ligand salt; for bidentate chelate mode the value of $\Delta\nu$ of complex is smaller than the value of $\Delta\nu$ of ligand salt and for bidentate bridge mode the value of $\Delta\nu$ of complex is slightly smaller than the value of $\Delta\nu$ of ligand salt [16,17]. The FT-IR of complexes' series with bza[−], ppa[−] and abse[−] ligands are shown in Fig. 1(a–c), respectively.

For all complexes containing the ligand bza[−] there are two different $\Delta\nu$ values, one of them is similar and the other is much smaller than the sodium ligand salt (Table 3). That fact indicates that bza[−] chemically binds to the lanthanides(III) ions by two coordination modes: bidentate chelate and bidentate bridge.

The coordination of the ligands ppa[−] or abse[−] were confirmed by the decrease on the frequency assigned to $\nu_{\text{as}}(\text{POO}^-)$ of the ppa[−] or $\nu_{\text{as}}(\text{SeOO}^-)$ of the abse[−] ligands when compared with the sodium salt of the respective ligands. Fig. 1b and c shows a splitting on the bands assigned to $\nu_{\text{s}}(\text{POO}^-)$ or $\nu_{\text{s}}(\text{SeOO}^-)$ when the ligand is bonded to lanthanide(III). This observation might be an indicative of two different coordination modes of the ligands ppa[−] or abse[−]. The same analysis previously used to figure out the coordination mode of the bza[−] ligand was also used for the ligands ppa[−] and abse[−] suggesting two coordination modes: bidentate bridging and bidentate chelating for the complexes. Once the stoichiometry and the coordination modes were established, the determination of the triplet state energy (T) is important in order to choose the lanthanide ions that can be used for efficient energy transfer.

The triplet state energy (T) of the ligands was determined by two ways: (i) fitting a tangent at the highest energy band edge of the phosphorescence or (ii) by the peak of the highest energy band that resulted from the deconvolution of the phosphorescence band. In both cases the time resolved phosphorescence emission spectra of analogous gadolinium(III) complexes were obtained

(shown in ESI Fig. S2). The energy values of the bza[−], ppa[−] and abse[−] triplet states are 25,641; 24,390 and 25,253 cm^{-1} , obtained by method (i) or 23,202; 22,026 and 22,727 cm^{-1} obtained by method (ii), respectively. The energy difference between the two values obtained is around 2000 cm^{-1} , but in all cases the value obtained is high enough to allow energy transfer from triplet states to the excited levels of lanthanides(III) ions ($^5\text{D}_{0,1}$ levels of Eu(III) and the $^5\text{D}_4$ level of Tb(III)).

In order to explore the luminescent properties of the europium (III) and terbium(III) complexes the excitation spectra were performed and are shown in Fig. 2A and C. There are broad bands assigned to ligand transitions (~ 280 and ~ 300 nm) and narrow bands assigned to the 4f–4f intraconfigurational transitions. In the case of the complexes containing the ligand abse[−] the intensity of the ligand band is always lower than 4f–4f transitions which might be an indicative of inefficient energy transfer from ligand to the lanthanide(III) ions.

The emission spectra of europium(III) complexes, Fig. 2B, show the characteristic transitions of this ion ($^5\text{D}_0 \rightarrow ^7\text{F}_j$, $j = 0, 1, 2, 3$ and 4). Because the first excited $^5\text{D}_0$ level is a non-degenerated emitting level it is possible to correlate the number of lines of the transition $^5\text{D}_0 \rightarrow ^7\text{F}_j$ with the point symmetry around europium(III) ions [1,18]. For [Eu(bza)₃(H₂O)₂] · 3/2(H₂O) and [Eu(abse)₃(H₂O)] complexes (Fig. 2B(a and c)) the number of lines of each $^5\text{D}_0 \rightarrow ^7\text{F}_j$ transition is higher than that for [Eu(ppa)₃] complex (Fig. 2B(b)). Therefore, the chemical environments around europium(III) ion in the [Eu(bza)₃(H₂O)₂] · 3/2(H₂O) and [Eu(abse)₃(H₂O)] complexes are less symmetric than that for the [Eu(ppa)₃] complex. For [Eu(bza)₃(H₂O)₂] · 3/2(H₂O) and [Eu(abse)₃(H₂O)] complexes the point symmetry may be approximated to a C_3 point group and for the [Eu(ppa)₃] complex it was not possible to correlate the number of lines for each transition with a specific symmetry point group. The relative high intensity of the $^5\text{D}_0 \rightarrow ^7\text{F}_1$ transition compared to the $^5\text{D}_0 \rightarrow ^7\text{F}_2$ transition of the [Eu(ppa)₃] complex (Fig. 2B(b)) is an indicative of a higher symmetry around the europium(III) ion in this complex. The presence of just one line for $^5\text{D}_0 \rightarrow ^7\text{F}_0$ for all complexes means that there is at least one symmetry site for europium(III) and that site is non-centro symmetric. In all emission spectra the $^5\text{D}_0 \rightarrow ^7\text{F}_2$ transitions are more intense than $^5\text{D}_0 \rightarrow ^7\text{F}_1$ ones, showing that the forced electric dipole and the dynamic coupling mechanisms are predominant in relation to magnetic dipole one, especially for [Eu(bza)₃(H₂O)₂] · 3/2(H₂O) (Fig. 2B(a)).

The calculation of the JO intensity parameters [19,20] (Ω_2 and Ω_4) of europium(III) complexes can help to understand the effects of the point symmetry, long range interactions and non-radiative rates (indirectly) on the optical properties. The JO parameters were calculated from europium(III) complexes' emission spectra and the equations and methodology used are described in ESI. The values of the JO intensity parameters (Ω_2 and Ω_4) and efficiency parameters ($1/\tau_{\text{rad}}$, A_{nrad} and η) of the europium(III) complexes are shown in the Table 4.

The Ω_2 intensity parameter can be correlated with the point symmetry around the europium(III) ion [21]. The Ω_2 values for the [Eu(bza)₃(H₂O)₂] · 3/2(H₂O) and [Eu(abse)₃(H₂O)] complexes (Table 4) are similar and they are higher than the Ω_2 value found for the [Eu(ppa)₃] complex. The lower value of Ω_2 parameter of the [Eu(ppa)₃] complex is an indicative of higher symmetry of the chemical environment around europium(III) ion in the latter complex. That result matches with the observation from the emission spectrum, which shows a smaller number of Stark levels of the $^5\text{D}_0 \rightarrow ^7\text{F}_j$ transitions and the relative high intensity of $^5\text{D}_0 \rightarrow ^7\text{F}_1$ transition compared to the $^5\text{D}_0 \rightarrow ^7\text{F}_2$ one for the complex [Eu(ppa)₃], (Fig. 2B(b)). The Ω_4 intensity parameter can be correlated with point symmetry around europium(III) ion and also to long range effects [22,23]. The higher values of Ω_4 intensity parameter observed for [Eu(bza)₃(H₂O)₂] · 3/2(H₂O) and

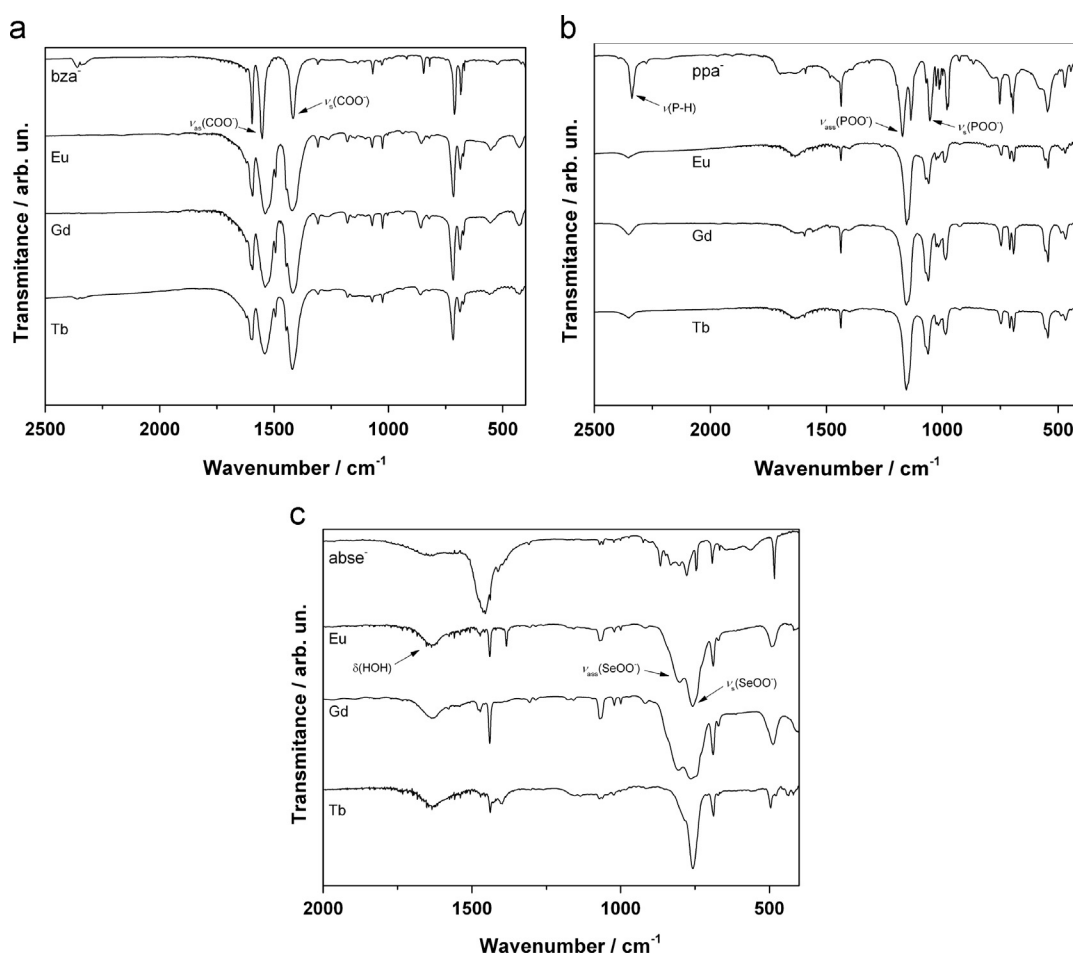


Fig. 1. FT-IR of lanthanide(III) complexes series in the region between 2000–400 cm^{-1} : (a) series containing bza^- ligand, (b) series containing ppa^- ligand and (c) series containing abse^- ligand.

Table 3

Wavenumber values of $\nu_{\text{as}}(\text{COO}^-)$, $\nu_{\text{s}}(\text{COO}^-)$ and $\Delta\nu(\text{COO}^-)$ for bza^- ligand and its complexes with lanthanides(III) ions.

Compounds	$\nu_{\text{as}} (\text{cm}^{-1})$	$\nu_{\text{s}} (\text{cm}^{-1})$	$\Delta\nu (\text{cm}^{-1})$	Coordination modes
bza^-	1553	1417	136	–
$[\text{Eu}(\text{bza})_3(\text{H}_2\text{O})_2] \cdot 3/2(\text{H}_2\text{O})$	1540/1519/1494	1422	118/97/72	Bridging/chelate
$[\text{Gd}(\text{bza})_3] \cdot (\text{H}_2\text{O})$	1540/1520/1495	1418	122/102/77	Bridging/chelate
$[\text{Tb}(\text{bza})_3(\text{H}_2\text{O})_2] \cdot 1/2(\text{H}_2\text{O})$	1541/1495	1495	120/74	Bridging/chelate

$[\text{Eu}(\text{abse})_3(\text{H}_2\text{O})]$ complexes (Table 5) may be correlated to long range interactions due to the formation of polymeric structures. A high value of Ω_4 parameter should be expected for the $[\text{Eu}(\text{ppa})_3]$ complex but the value is very low which could be explained by the low intensity of $^5\text{D}_0 \rightarrow ^7\text{F}_4$. As we can see the values of τ_{rad} (Table 4) calculated using the Judd–Ofelt theory ($\tau_{\text{rad}}^{\text{a}}$) are in very good agreement with the ones obtained using the emission spectra data ($\tau_{\text{rad}}^{\text{b}}$) considering an error around 15% for the values obtained by Judd–Ofelt theory according to Verheeven and co-workers [24].

The energy of the $^5\text{D}_0 \rightarrow ^7\text{F}_0$ transition (E_{00}) might be correlated with the covalence between Eu–L bonds [25–27]. A decrease in energy, or a redshift, of this transition means an increase in the covalence degree of Eu–L bonds. For the complexes described in this work the bza^- and ppa^- ligands may promote similar covalence degree of Ln–O bonds because of similarity between their E_{00} energy values (Table 4). On the other hand, the abse^- ligand has the ability to increase the covalence degree of Ln–O bonds (Table 4). The only difference between the ligand abse^- and

the others is the lone pair localized on the selenium atom. Probably the lone pair contributes somehow to increase the electron density on the SeOO^- ligand group and then the covalence of the Ln–O (acid) bonds.

The emission decay lifetime values of the $^5\text{D}_0$ emitting level of the europium(III) complexes may be correlated with the non-radiative decay caused by the multi-phonon processes due to the presence of N–H, O–H or/and C–H oscillators. In this specific case, the number of coordinated water molecules and the rigidity of the complexes' structure may be important factors that can influence the emission lifetime values. As shown in Table 5 the emission lifetime values of the $^5\text{D}_0$ emitting level of the $[\text{Eu}(\text{ppa})_3]$ complex is the highest among the complexes. This result may be directly correlated with the absence of water molecules in the coordination sphere and high rigidity of structure due to the possible formation of a polymeric structure. Similar results were reported by Stucchi and co-workers [9,10] for the complexes $[\text{Eu}(\text{dpp})_3]$ and $[\text{Gd}(\text{dpp})_3]$ doped with europium(III) (where dpp =diphenylphosphinate). The $[\text{Tb}(\text{ppa})_3]$ has the longest emission lifetime value among the synthesized

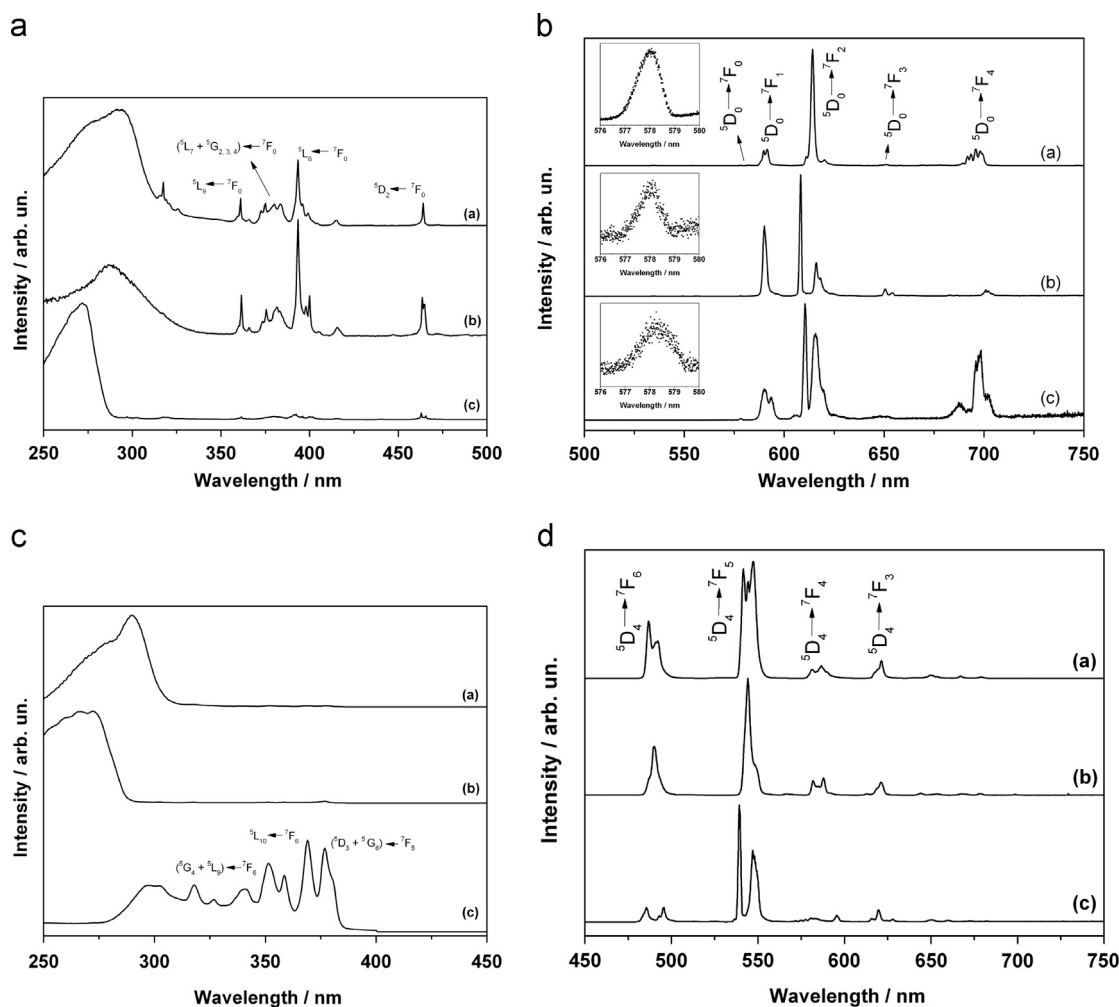


Fig. 2. Emission and excitation spectra of the lanthanide complexes obtained at ~ 77 K and ~ 298 K, respectively. (A) Excitation spectra of europium(III) complexes, (B) emission spectra of europium(III) complexes, (C) excitation spectra of terbium(III) complexes and (D) emission spectra of terbium(III) complexes. In all cases (a–c) are the complexes containing the ligands bza, ppa and abse, respectively.

Table 4
Values of the JO intensity parameters (Ω_2), spontaneous emission rates (A), quantum efficiency (η) and energy (E_{00}) of the $^5D_0 \rightarrow ^7F_0$ transition of the europium(III) complexes.

Complexes	Ω_2 (10^{-20} cm^2)	Ω_4 (10^{-20} cm^2)	τ_{rad}^a (ms)	τ_{rad}^b (ms)	A_{nrad} (s^{-1})	η (%)	E_{00} (cm^{-1})
[Eu(bza) ₃ (H ₂ O) ₂] · 3/2(H ₂ O)	9.9	7.1	2.21	2.21	2048.4	18	17,270
[Eu(ppa) ₃]	3.4	0.8	1.96	2.44	128.1	56	17,267
[Eu(abse) ₃ (H ₂ O)]	8.9	12.9	6.08	6.67	1449.8	26	17,248

^a Values obtained using the Judd–Ofelt theory.

^b Values obtained using the emission spectrum data.

complexes because 5D_4 emitting level of the terbium(III) ions is energetically higher than the 5D_0 emitting level of europium(III) ions with the rate of non-radiative process being less effective for the terbium(III) complex.

In a recent paper, Ferreira et al. [28] reported a correlation between the emission lifetime of the 5D_0 emitting level and the excitation wavelengths. In order to verify if the different excitation wavelengths lead to different ways to populate/depopulate the emitting level, the 5D_0 emission lifetime was measured under ligand bands or f–f excitations, (Table 5). Table 5 shows nearly the same lifetime values under different excitations. These results mean that the 5D_0 emission lifetime is independent of the excitation wavelength. In other

words, in this case, there are no different non-radiative routes that can be activated when the excitation wavelength is changed.

The number of coordinated water molecules can be estimated by Eq. (1) [29]. The calculated and experimental values of the number of coordinated water molecules in the complexes are shown in Table 6.

$$n = 1.11 \left[\frac{1}{\tau(\text{H}_2\text{O})} - \frac{1}{\tau(\text{D}_2\text{O})} - 0.31 \right] \quad (1)$$

where $\tau(\text{H}_2\text{O})$ and $\tau(\text{D}_2\text{O})$ are the emission lifetime values of the 5D_0 emitting level of the complexes containing coordinated water or D₂O molecules, respectively. The emission lifetime of europium(III)

Table 5Emission lifetime values of the 5D_0 emitting level obtained at different excitation wavelengths.

Complexes	τ (ms)	λ_{exc} (nm)
[Eu(bza) ₃ (H ₂ O) ₂] · 3/2(H ₂ O)	0.44	276.0
	0.42	292.8
	0.45	393.5
	0.47	464.0
[Eu(ppa) ₃]	4.05	265.0
	4.02	271.7
	3.98	392.5
	3.99	463.0
[Eu(abse) ₃ (H ₂ O)]	0.58	287.0
	0.57	393.5
	0.56	464.0
[Tb(bza) ₃ (H ₂ O) ₂] · 1/2(H ₂ O)	0.90	280.0
[Tb(ppa) ₃]	6.42	368.6
[Tb(abse) ₃ (H ₂ O)]	0.70	270.0

Table 6Comparison between the number of coordinated water molecules (n) of the complexes obtained experimentally from TG analysis (n_{exp}) and obtained from Eq. (1) (n_{calc}).

Complexes	n_{exp}	n_{calc}
[Eu(bza) ₃ (H ₂ O) ₂] · 3/2(H ₂ O)	2	1.9
[Eu(ppa) ₃]	0	0
[Eu(abse) ₃ (H ₂ O)]	1	1.3

Table 7Values of absolute quantum yield of the europium (III) complexes obtained with the excitation wavelength centered in f–f transition ($^5D_2 \leftarrow ^7F_0$).

Complexes	ϕ_{Ln}^{Ln} (%)
[Eu(bza) ₃ (H ₂ O) ₂] · 3/2(H ₂ O)	11.5 ± 0.7
[Eu(ppa) ₃]	43.5 ± 3.1
[Eu(abse) ₃ (H ₂ O)]	9.9 ± 1.2

coordinated to D₂O molecules ($\tau(D_2O)$), may be obtained from the radiative spontaneous emission rate (A_{rad}) that can be calculated from the experimental emission spectrum and therefore τ_{rad} can be used in Eq. (1) substituting $\tau(D_2O)$. The number of coordinated water molecules for all europium(III) complexes, obtained from Eq. (1), matches very well with the experimental ones obtained from TG analysis (Table 3).

The absolute emission quantum yields of the europium(III) complexes were measured using the excitation centered on intraconfigurational 4f–4f transition ($^5D_2 \leftarrow ^7F_0$). The values of the absolute quantum yields are shown in Table 7. For europium(III) complexes, the value of absolute quantum yield can be strongly correlated with the number of coordinated water molecules that represents a non-radiative route and therefore is a factor for decreasing the absolute quantum yield as they also do for emission lifetime values. The [Eu(ppa)₃] complex has the highest value of absolute emission quantum yield. The low non-radiative rates from the 5D_0 emitting level due to the absence of coordinated

water molecules, its polymeric structure and also the values of back energy transfer rates involved on the depopulation ($^5D_1 \rightarrow T$ and $^5D_0 \rightarrow T$) of the $^5D_{0,1}$ level (Tables 10–12), which will be discussed later (Tables 12–14), suggest that the [Eu(ppa)₃] complex has the lowest energy back transfer than the other complexes. This should be one of the key factors for the highest quantum yield among the complexes. The quantum yields of terbium(III) complexes were not determined due to the low emission intensity when those complexes were excited in $^5L_{10} \leftarrow ^7F_6$ intraconfigurational 4f–4f transition.

For a better understanding about the transfer rates it is necessary first to obtain the polar spherical coordinates. For this purpose the ground state geometries of europium(III) complexes were obtained using Sparkle/AM1 [12], Sparkle/PM3 [13] or Sparkle/PM6 [14] implemented in MOPAC2009 software [15] in order to determine the coordination polyhedron around the europium(III). Figs. 3–5 show a comparison among the ground state geometries obtained by these methods. Due to the polymeric nature of complexes the strategy to calculate the ground state geometries was the same as that used by Freire et al. [30]. Three metallic centers were drawn: the metal on the center has its coordination sphere filled with the ligands and water molecules (if applicable); the two metals in each side have the coordination sphere filled with the chelates ligands and water molecules. In other words the bridging ligands connect the metal on the center with the metals on both sides. The coordination modes of the bza[−], ppa[−] and abse[−] ligands in the complexes were first analyzed by FT-IR. Additional information about different coordination modes of the bza[−], ppa[−] and abse[−] ligands were obtained by simulating the ground-state geometries using the Sparkle model and test if the calculated JO intensity parameters obtained from the ground-state geometries data approach the experimental ones obtained from the emission spectra of europium (III) complexes (Table 9).

Using this strategy, the coordination modes for the bza[−] ligand matches those found by FT-IR. It was also possible to verify the two coordination modes for ppa[−] ligand in the [Eu(ppa)₃] and for abse[−] ligand in the [Eu(abse)₃(H₂O)] complexes – bidentate bridging and bidentate chelate. Additionally, a search was done in the Cambridge Structural Database [31] in order to find structures of complexes containing the ligands ppa[−] or abse[−]. For the ligand abse[−], structures with Sn [32] or Mn [33] were found and for the ppa[−] ones structures with Ru [34], Mn [35,36], Al [37], and Sb [38] were found. Just two coordination modes were found in those structures: monodentate and bidentate bridging, that to some extent is in accordance with the prediction of the structures of the [Eu(ppa)₃] and [Eu(abse)₃(H₂O)] complexes having the bidentate bridging coordination mode. The bidentate chelate coordination mode in the complexes may be reasonable since the lanthanide(III) ions usually have a higher coordination number (6–12) than the metal ions cited above.

The values of polarizability (α) and charge factors (g) (Table 8) of the ligands bonded to the europium(III) ions were obtained using the polar spherical coordinates of the ground state geometry obtained from Sparkle/AM1, Sparkle/PM3 or Sparkle/PM6 calculation (see ESI for details) and from the intensity parameters experimentally obtained (Table 4). The equations used for this purpose are described in ESI and in the literature [39]. The polarizability (α) and the charge factor (g) are determined by adjusting the JO intensity parameters obtained theoretically with the experimental ones.

The values of the Ω_2 obtained from Sparkle/AM1, Sparkle/PM3 and Sparkle/PM6 (Table 9) are in agreement with experimental ones (Table 4) meaning that the coordination polyhedral is well described by the three methods. However, the Ω_4 values obtained theoretically do not match with experimental ones. Davolos et al. [22] and Freire et al. [40] have observed the same trend for the [Eu

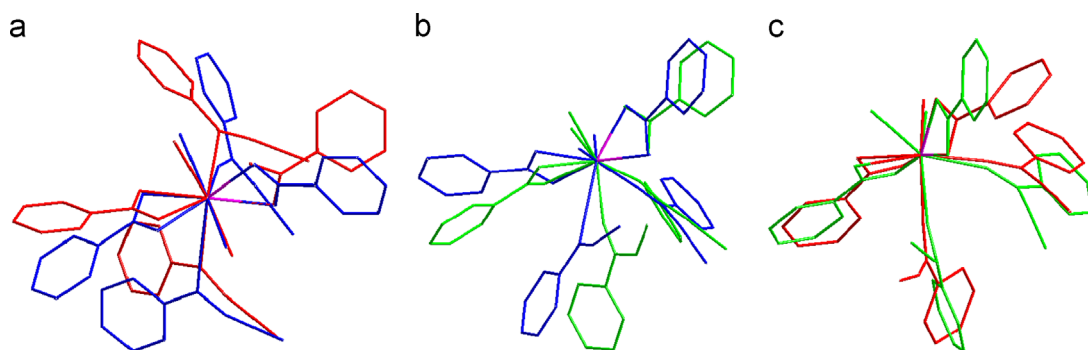


Fig. 3. Comparison between the ground state geometries of the $[\text{Eu}(\text{bza})_3(\text{H}_2\text{O})_2] \cdot 3/2(\text{H}_2\text{O})$ complex being Sparkle/AM1 (blue), Sparkle/PM3 (red) and Sparkle/PM6 (green). (a) Sparkle/AM1 and Sparkle/PM3, (b) Sparkle/AM1 and Sparkle/PM6, and (c) Sparkle/PM3 and Sparkle/PM6. (For interpretation of the references to color in this figure legend, the reader is referred to the web version of this article.)

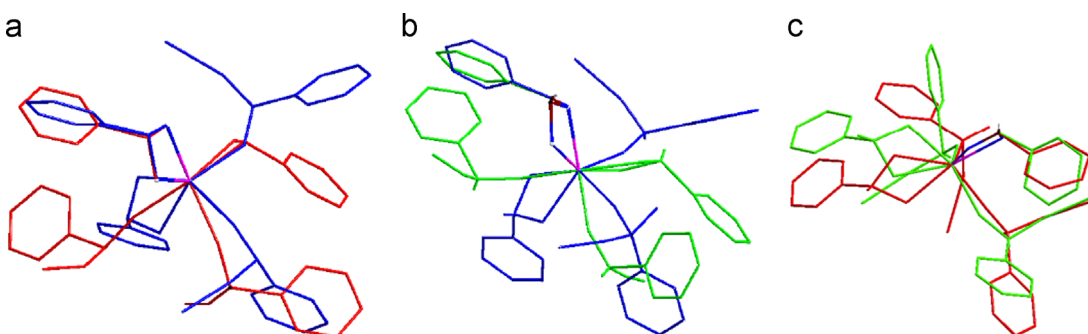


Fig. 4. Comparison between the ground state geometries of the $[\text{Eu}(\text{ppa})_3]$ complex being Sparkle/AM1 (blue), Sparkle/PM3 (red) and Sparkle/PM6 (green). (a) Sparkle/AM1 and Sparkle/PM3, (b) Sparkle/AM1 and Sparkle/PM6, and (c) Sparkle/PM3 and Sparkle/PM6. (For interpretation of the references to color in this figure legend, the reader is referred to the web version of this article.)

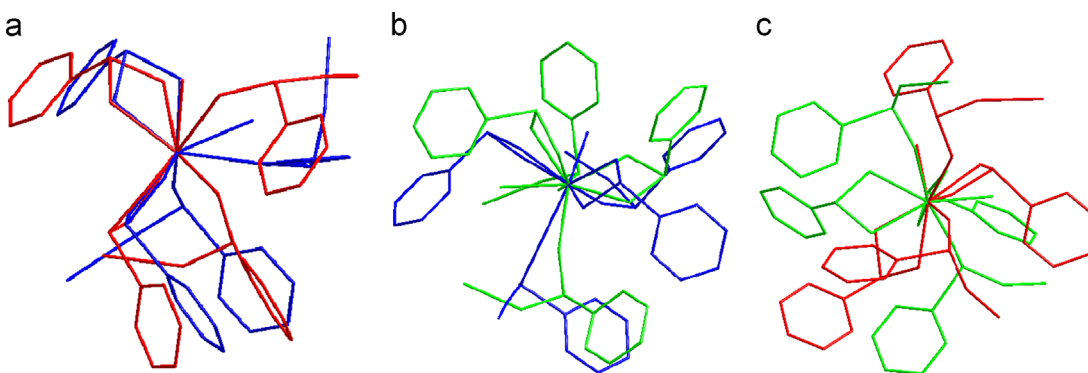


Fig. 5. Comparison between the ground state geometries of the $[\text{Eu}(\text{abse})_3(\text{H}_2\text{O})]$ complex being Sparkle/AM1 (blue), Sparkle/PM3 (red) and Sparkle/PM6 (green). (a) Sparkle/AM1 and Sparkle/PM3, (b) Sparkle/AM1 and Sparkle/PM6, and (c) Sparkle/PM3 and Sparkle/PM6. (For interpretation of the references to color in this figure legend, the reader is referred to the web version of this article.)

Table 8

Charge factors (g) and polarizability (α) obtained with Sparkle for complexes.

Complexes	g_1 (acid)			g_2 (water)			α_1 (acid)			α_2 (water)		
	AM1	PM3	PM6	AM1	PM3	PM6	AM1	PM3	PM6	AM1	PM3	PM6
$[\text{Eu}(\text{bza})_3(\text{H}_2\text{O})_2] \cdot 3/2(\text{H}_2\text{O})$	1.0	1.0	1.0	0.5	0.5	0.5	2.90	3.11	3.85	0.1	0.1	0.1
$[\text{Eu}(\text{ppa})_3]$	1.0	1.0	1.0	–	–	–	1.31	2.06	2.30	–	–	–
$[\text{Eu}(\text{abse})_3(\text{H}_2\text{O})]$	1.0	1.0	1.0	0.5	0.5	0.5	2.52	2.65	2.77	0.1	0.1	0.1

(bmdm)₃(tppo)] and $[\text{Eu}(\text{phen})_2(\text{NO}_3)_3]$ complexes. Probably that discordance between experimental and theoretical Ω_4 values is due to the long range interactions that play a special role in polymeric complexes. The calculated polarizability values should reflect the covalence degree of Eu–L bonds. Experimentally there is a correlation between the energy of the $^5\text{D}_0 \rightarrow ^7\text{F}_0$ transition and

the degree of covalence [25–27]. The energy values of the $^5\text{D}_0 \rightarrow ^7\text{F}_0$ transition (E_{00} , Table 4) indicate that the covalence degree is higher for $[\text{Eu}(\text{abse})_3(\text{H}_2\text{O})]$ complex and the other two complexes ($[\text{Eu}(\text{bza})_3(\text{H}_2\text{O})_2] \cdot 3/2(\text{H}_2\text{O})$ and $[\text{Eu}(\text{ppa})_3]$) have nearly the same degree of covalence. The calculated polarizability values show that the complex with bza[–] ligand should have the higher degree of

Table 9

Intensity parameters (Ω_2 , Ω_4 and Ω_6) obtained experimentally and theoretically using the polar spherical coordinates of the ground state geometry provided by Sparkle method.

Complexes	Ω_2 (10^{-20} cm ²)			$(\Omega_2)_{\text{exp}}$ (10^{-20} cm ²)	Ω_4 (10^{-20} cm ²)			$(\Omega_4)_{\text{exp}}$ (10^{-20} cm ²)	Ω_6 (10^{-20} cm ²)		
	AM1	PM3	PM6		AM1	PM3	PM6		AM1	PM3	PM6
[Eu(bza) ₃ (H ₂ O) ₂] · 3/2(H ₂ O)	9.9	9.9	9.9	9.9	0.82	0.63	1.08	7.1	0.15	0.04	0.07
[Eu(ppa) ₃]	3.4	3.4	13.4	3.4	0.10	0.17	0.07	0.8	0.22	0.14	0.15
[Eu(abse) ₃ (H ₂ O)]	8.9	8.9	8.9	8.9	0.46	0.44	0.39	12	0.18	0.06	0.06

Table 10

Values of energy transfer and back transfer rates among the triplet state (T) and $^5D_{0,1}$ levels of the europium complexes calculated from ground state geometries provided by Sparkle/AM1.

Complexes	T → $^5D_1^a$	T → $^5D_1^b$	5D_1 → T ^a	5D_1 → T ^b	T → $^5D_0^a$	T → $^5D_0^b$	5D_0 → T ^a	5D_0 → T ^b
[Eu(bza) ₃ (H ₂ O) ₂] · 3/2(H ₂ O)	4.6×10^8	2.5×10^9	1.2×10^{-5}	7.2	8.0×10^7	7.8×10^8	4.4×10^{-10}	4.8×10^{-4}
[Eu(ppa) ₃]	7.1×10^8	2.5×10^9	7.0×10^{-3}	2.0×10^3	1.7×10^8	1.0×10^9	3.5×10^{-7}	0.2
[Eu(abse) ₃ (H ₂ O)]	2.7×10^8	1.4×10^9	4.4×10^{-5}	38	5.2×10^7	4.7×10^8	1.8×10^{-9}	2.8×10^{-3}

^a Using the triplet state energy value obtained by fitting a tangent to the band edge of the phosphorescence band.

^b Using the peak of the highest energy band (0-0 phonon) obtained from the deconvolution of the phosphorescence spectrum.

Table 11

Values of energy transfer and back transfer rates among the triplet state (T) and $^5D_{0,1}$ levels of the europium complexes calculated from ground state geometries provided by Sparkle /PM3.

Complexes	T → $^5D_1^a$	T → $^5D_1^b$	5D_1 → T ^a	5D_1 → T ^b	T → $^5D_0^a$	T → $^5D_0^b$	5D_0 → T ^a	5D_0 → T ^b
[Eu(bza) ₃ (H ₂ O) ₂] · 3/2(H ₂ O)	4.8×10^8	2.6×10^9	1.2×10^{-5}	7.4	8.3×10^7	8.0×10^8	4.6×10^{-10}	4.9×10^{-4}
[Eu(ppa) ₃]	3.9×10^8	1.4×10^9	3.9×10^{-3}	1.1×10^3	9.1×10^7	5.7×10^8	1.9×10^{-7}	0.1
[Eu(abse) ₃ (H ₂ O)]	3.2×10^8	1.6×10^9	5.1×10^{-5}	44	6.1×10^7	5.5×10^8	2.1×10^{-9}	3.3×10^{-3}

^a Using the triplet state energy value obtained by fitting a tangent to the band edge of the phosphorescence band.

^b Using the peak of the highest energy band (0-0 phonon) obtained from the deconvolution of the phosphorescence spectrum.

Table 12

Values of energy transfer and back transfer rates among the triplet state (T) and $^5D_{0,1}$ levels of the europium complexes calculated from ground state geometries provided by Sparkle /PM6.

Complexes	T → $^5D_1^a$	T → $^5D_1^b$	5D_1 → T ^a	5D_1 → T ^b	T → $^5D_0^a$	T → $^5D_0^b$	5D_0 → T ^a	5D_0 → T ^b
[Eu(bza) ₃ (H ₂ O) ₂] · 3/2(H ₂ O)	4.8×10^8	2.6×10^9	1.2×10^{-5}	7.4	8.3×10^7	8.0×10^8	4.6×10^{-10}	4.9×10^{-4}
[Eu(ppa) ₃]	5.2×10^8	1.9×10^9	5.1×10^{-3}	1.4×10^3	1.2×10^8	7.4×10^8	2.6×10^{-7}	0.1
[Eu(abse) ₃ (H ₂ O)]	2.3×10^8	1.2×10^9	3.7×10^{-5}	32	4.4×10^7	4.0×10^8	1.5×10^{-9}	2.4×10^{-3}

^a Using the triplet state energy value obtained by fitting a tangent to the band edge of the phosphorescence band.

^b Using the peak of the highest energy band (0-0 phonon) obtained from the deconvolution of the phosphorescence spectrum.

covalence and the ppa[−] the smaller one. The non-correlation between the experimental and theoretical data may be caused by misleading propositions of the polar spherical coordinates of the oxygen ions bonded to the lanthanide once polymeric complexes are difficult to be simulated at long range [30] that may also be one cause for the difference among the obtained Ω_4 values.

In a lanthanide(III) complex the organic part has the function of absorbing energy in the UV region and transfers it to the lanthanide ion. The energy transfer rates of the europium complexes were estimated considering the energy transfer from the triplet state (T) to the $^5D_{0,1}$ levels and using the equations reported by Malta and co-workers [41–43]. As a comparison the triplet state energy values determined by the two methodologies were used, as discussed in the luminescence section; Tables 10–12 show the values of calculated energy transfer and back transfer rates.

The population of the excited levels of the europium(III) ion and the theoretical quantum yield were calculated using the adequate kinetics equations described in ESI and in literature [41–43]. The calculated values are shown in Table 13.

Tables 10–12 show that for different energy values of the triplet state, obtained by the different methods, the energy transfer rates (T → $^5D_{0,1}$) increase in average one order of magnitude and the back energy transfer rates ($^5D_{0,1}$ → T) increase in average 10^5 times for the same complex. This is an interesting observation for planning future efficient emitting complexes. This data shows, at least in this case, that the energy transfer rates are less affected by small changes in the triplet state energy. Probably that happens because of the energy gap between the triplet state and the 5D_1 or 5D_0 levels (≥ 2500 cm^{−1}). However, even considering the increase of back energy transfer rates, the population of emitting level and the theoretical quantum yield (Tables 13 and 14) are not affected significantly as a function of the triplet state energy considered in this work for these complexes. An explanation for that could be the high value of energy transfer rates when compared with the back transfer ones (10^8 versus 10^2 , respectively) and probably the energy gap between the triplet state and emitting level is high enough to minimize the difference of the triplet state energy obtained from the two different methods. In general the emission

Table 13Population of electronic states of Eu^{3+} ($^5\text{D}_1$ and $^5\text{D}_0$) and theoretical quantum yield (q) calculated from ground state geometries provided by Sparkle^a.

Complexes	$N(^5\text{D}_1)$			$N(^5\text{D}_0)$			q (%)		
	AM1	PM3	PM6	AM1	PM3	PM6	AM1	PM3	PM6
[Eu(bza) ₃ (H ₂ O) ₂] · 3/2(H ₂ O)	1.6×10^{-3}	1.6×10^{-3}	1.6×10^{-3}	0.80	0.80	0.80	15	15	15
[Eu(ppa) ₃]	2.2×10^{-4}	2.2×10^{-4}	2.3×10^{-4}	0.97	0.97	0.97	54	54	54
[Eu(abse) ₃ (H ₂ O)]	1.3×10^{-3}	5.2×10^{-4}	1.3×10^{-3}	0.85	0.85	0.85	18	18	18

^a Using the triplet state energy value obtained by fitting a tangent to the band edge of the phosphorescence band.**Table 14**Population of electronic states of Eu^{3+} ($^5\text{D}_1$ and $^5\text{D}_0$) and theoretical quantum yield (q) calculated from ground state geometries provided by Sparkle^a.

Complexes	$N(^5\text{D}_1)$			$N(^5\text{D}_0)$			q (%)		
	AM1	PM3	PM6	AM1	PM3	PM6	AM1	PM3	PM6
[Eu(bza) ₃ (H ₂ O) ₂] · 3/2(H ₂ O)	1.5×10^{-3}	1.5×10^{-3}	1.5×10^{-3}	0.80	0.80	0.80	15	15	15
[Eu(ppa) ₃]	2.0×10^{-4}	2.0×10^{-4}	1.9×10^{-4}	0.97	0.97	0.97	54	54	54
[Eu(abse) ₃ (H ₂ O)]	1.1×10^{-3}	1.1×10^{-3}	1.1×10^{-3}	0.85	0.85	0.85	18	18	18

^a Using the peak of the highest energy band (0–0 phonon) obtained from the deconvolution of the phosphorescence spectrum.

quantum yields of lanthanide(III) complexes are moderated by the energy transfer and back transfer rates, asymmetry and presence or not of non-radiative routes such as the O–H oscillator. In the present case the complexes show higher transfer rate from ligand to metal when compared with the values in the literature [22] and low back transfer rates leading to a high population of the $^5\text{D}_0$ emitting level of europium(III). For the [Eu(ppa)₃] complex the absence of water molecules in the first coordination sphere is a key factor for the high observed emission quantum yield (Tables 13 and 14).

6. Conclusions

The coordination modes of the bza[−] ligand were determined by FT-IR measurements. It was possible to use the same methodology to propose the coordination modes of the ppa[−] ligand. The coordination modes are practically independent of the ligands functional group, however, in the case of europium(III) complexes the functional groups showed an important influence on the luminescent properties. The [Eu(abse)₃(H₂O)] complex shows the higher degree of covalence (Eu–O). The lone pair of the selenium atom contributes for the increase of the covalence between Eu–O bonds. However the [Ln(abse)₃(H₂O)] complexes have an inefficient antenna effect, verified by the low values of absolute emission quantum yields.

Two methodologies were used to obtain the triplet state energy and the difference between them is at least 2000 cm^{-1} . The energy transfer and back transfer rates were calculated using the two triplet state energies obtained and it is possible to verify that the values of energy transfer rates from the ligands' states to europium(III) $^5\text{D}_1$ and $^5\text{D}_0$ levels have small influence with relation to the triplet state energy. On the other hand the back energy transfer rates increases $\sim 10^5$ times. The different values of the transfer rates do not have a big influence on the population of the $^5\text{D}_0$ emitting level of europium(III) and neither the theoretical quantum yield due to the high energy gap between the triplet state energy level and the $^5\text{D}_0$ emitting level. The [Ln(ppa)₃] complexes are anhydrous polymers having the highest point symmetry around the europium(III) ion, emission quantum efficiency and absolute quantum yield. The high values of the quantum efficiency and absolute quantum yield for the [Eu(ppa)₃] complex is a combination of high energy transfer rates and low energy back transfer rates and the absence of non-

radiative decay routes, such as water molecules in coordination sphere.

The energy transfer rates calculation provided a way to understand the implications of the triplet state energy changes in the theoretical values of quantum yield and to understand the higher quantum yield values observed for the [Eu(ppa)₃] complex. All experimental and theoretical values were used to investigate the influence of carbon, phosphorous and selenium atoms on the coordination modes, on the nature of the chemical bond between the ligands and the lanthanides, and on the luminescent properties.

Acknowledgments

JHSM is indebted to CNPq for a Ph.D. fellowship. FAS and ALBF are indebted to CNPq, CAPES and FAPESP (Grant no. 2008/53868-0) for financial support. The authors would like to thank Prof. Dr. Ricardo Freire (UFS) for providing the Mathcad routine for Judd–Ofelt theoretical parameters calculation, energy transfer rates and population of the lanthanide electronic levels, and also Prof. Dr. Alfredo M. Simas (UFPE) for helping with computational facilities and the Laboratory of Advanced Optical Spectroscopy (LMEOA/IQ-UNICAMP/FAPESP Grant no. 2009/54066-7). This work is a contribution of the National Institute of Science and Technology in Complex Functional Materials (CNPq-MCT/FAPESP).

Appendix A. Supporting information

Supplementary data associated with this article can be found in the online version at <http://dx.doi.org/10.1016/j.jlumin.2014.03.071>.

References

- [1] J.-C.G. Bünzli, S.V. Eliseeva, Basics of lanthanide photophysics, in: P. Hänninen, H. Härmä, O.S. Wolfbeis (Eds.), *Lanthanide Luminescence: Photophysical, Analytical and Biological Aspects*, Springer-Verlag, Berlin, 2011, p. 3 (Chapter 1).
- [2] K. Binnemans, *Chem. Rev.* 109 (2009) 4283.
- [3] K. Binnemans, Rare-earth beta-diketones, in: K.A. Gschneider, J.-C.G. Bünzli, V.K. Pecharsky (Eds.), *Handbook on the Physics and Chemistry of Rare Earths*, 35, Elsevier, Amsterdam, 2005, p. 107 (Chapter 225).
- [4] A. D'Aléo, F. Pointillart, L. Ouahab, C. Andraud, O. Maury, *Coord. Chem. Rev.* 256 (2012) 1604.
- [5] J. Andres, A.-S. Chauvin, *Phys. Chem. Chem. Phys.* 15 (2013) 15981.
- [6] L. Smentek, A. Kedzior, *J. Lumin.* 130 (2010) 1154.

- [7] S. Chen, R.-Q. Fan, C.-F. Sun, P. Wang, Y.-L. Yang, Q. Su, Y. Mu, *Cryst. Growth Des.* 12 (2012) 1337.
- [8] S. Nayak, G.E. Kostakis, C.E. Anson, A.K. Powell, *CrystEngComm* 12 (2010) 3008.
- [9] E.B. Stucchi, S.L. Scarpari, M.A.C. Santos, S.R.A. Leite, J. *Alloys Compd.* 275–277 (1998) 89.
- [10] S.L. Scarpari, E.B. Stucchi, J. *Alloys Compd.* 323–324 (2001) 740.
- [11] A.P. Souza, L.C.V. Rodrigues, H.F. Brito, S.A. Junior, O.L. Malta, J. *Lumin.* 130 (2010) 181.
- [12] R.O. Freire, G.B. Rocha, A.M. Simas, *Inorg. Chem.* 44 (2005) 3299.
- [13] R.O. Freire, G.B. Rocha, A.M. Simas, J. *Braz. Chem. Soc.* 20 (2009) 1638.
- [14] R.O. Freire, A.M. Simas, J. *Chem. Theory Comput.* 6 (2010) 2019.
- [15] J.J.P. Stewart, *MOPAC 2009 Manual*, Stewart Computational Chemistry, Colorado Springs, USA, 2009.
- [16] G.B. Deacon, R.J. Phillips, *Coord. Chem. Rev.* 33 (1980) 227.
- [17] K. Nakamoto, *Infrared and Raman Spectra of Inorganic and Coordination Compounds – Part B: Applications in Coordination, Organometallic, and Bioinorganic Chemistry*, John Wiley, New York, 1997.
- [18] P.A. Tanner, in: P. Hänninen, H. Härmä, O.S. Wolfbeis (Eds.), *Lanthanide Luminescence in Solids*, Springer-Verlag, Berlin, 2011, p. 203.
- [19] B.R. Judd, *Phys. Rev.* 127 (1962) 750.
- [20] G.S. Ofelt, J. *Chem. Phys.* 37 (1962) 511.
- [21] E.M. Rodrigues, E.R. Souza, J.H.S.K. Monteiro, R.D.L. Gaspar, I.O. Mazali, F.A. Sigoli, J. *Mater. Chem.* 22 (2012) 24109.
- [22] J.H.S.K. Monteiro, R.D. Adati, M.R. Davolos, J.R.M. Vicenti, R.A. Burrow, *New J. Chem.* 35 (2011) 1234.
- [23] R.A.S. Ferreira, S.S. Nobre, C.M. Granadeiro, H.I.S. Nogueira, L.D. Carlos, O.L. Malta, J. *Lumin.* 121 (2006) 561.
- [24] M.H.V. Werts, R.T.F. Jukes, J.W. Verhoeven, *Phys. Chem. Chem. Phys.* 4 (2002) 1542.
- [25] S.T. Frey, W. DeW Horrocks, *Inorg. Chim. Acta* 229 (1995) 383.
- [26] O.L. Malta, H.J. Batista, L.D. Carlos, *Chem. Phys.* 282 (2002) 21.
- [27] L.D. Carlos, O.L. Malta, R.Q. Albuquerque, *Chem. Phys. Lett.* 415 (2005) 238.
- [28] R.A.S. Ferreira, M. Nolasco, A.C. Roma, R.L. Longo, O.L. Malta, L.D. Carlos, *Chem. Eur. J.* 18 (2012) 12130.
- [29] L.D. Carlos, R.A.S. Ferreira, V.Z. Bermudez, S.J.L. Ribeiro, *Adv. Mater.* 21 (2009) 509.
- [30] M.O. Rodrigues, N.B.C. Júnior, C.A. Simone, A.A.S. Araújo, A.M. Brito-Silva, F.A.A. Paz, M.E. Mesquita, S.A. Júnior, R.O. Freire, J. *Phys. Chem. B* 112 (2008) 4204.
- [31] F.H. Allen, *Cambridge structural database*, Version 5.31, November 2009, *Acta Crystallogr. Sect. B: Struct. Sci.* 58 (2002) 380.
- [32] V. Chandrasekhar, M.G. Muralidhara, K.R.J. Thomas, E.R.T. Tiekink, *Inorg. Chem.* 31 (1992) 4707.
- [33] N.E. Chakov, W. Wernsdorfer, K.A. Abboud, G. Christou, *Inorg. Chem.* 43 (2004) 5919.
- [34] M. McCann, E. Murphy, C. Cardin, M. Convery, *Polyhedron* 12 (1993) 1725.
- [35] S.M. Taylor, R.D. McIntosh, C.M. Beavers, S.J. Teat, S. Piligkos, S.J. Dalgarno, E.K. Brechin, *Chem. Commun.* 47 (2011) 1440.
- [36] K. Bernot, J. Luzon, R. Sessoli, A. Vindigni, J. Thion, S. Richter, D. Leclercq, J. Larionova, A. Van der Lee, J. *Am. Chem. Soc.* 130 (2008) 1619.
- [37] Y. Wang, S. Parkin, D. Atwood, *Chem. Commun.* 19 (2000) 1799.
- [38] T. Svoboda, R. Jambor, A. Ruzicka, Z. Padelkova, M. Erben, L. Dostal, *Eur. J. Inorg. Chem.* (2010) 5222.
- [39] G.F. Sá, O.L. Malta, C.M. Donegá, A.M. Simas, R.L. Longo, P.A. Santa-Cruz, E.F.S. Júnior, *Coord. Chem. Rev.* 196 (2000) 165.
- [40] J.D.L. Dutra, R.O. Freire, J. *Photochem. Photobiol. A* 256 (2013) 29.
- [41] O.L. Malta, F.R.G. Silva, *Spectrochim. Acta Part A* 54 (1998) 1593.
- [42] O.L. Malta, F.R.G. Silva, R. Longo, *Chem. Phys. Lett.* 307 (1999) 518.
- [43] O.L. Malta, J. *Non-Cryst. Solids* 354 (2008) 4770.